

## On anisotropic versions of three-dimensional pentamode metamaterials

Muamer Kadic<sup>1,3</sup>, Tiedo Bückmann<sup>1</sup>, Robert Schittny<sup>1</sup>  
and Martin Wegener<sup>1,2</sup>

<sup>1</sup> Institute of Applied Physics, Karlsruhe Institute of Technology (KIT),  
D-76128 Karlsruhe, Germany

<sup>2</sup> Institute of Nanotechnology, Karlsruhe Institute of Technology (KIT),  
Hermann-von-Helmholtz-Platz 1, D-76344 Eggenstein-Leopoldshafen,  
Germany

E-mail: [muamer.kadic@kit.edu](mailto:muamer.kadic@kit.edu)

*New Journal of Physics* **15** (2013) 023029 (12pp)

Received 20 November 2012

Published 18 February 2013

Online at <http://www.njp.org/>

doi:10.1088/1367-2630/15/2/023029

**Abstract.** Pentamode materials are artificial solids with elastic properties that approximate those of isotropic liquids. The corresponding three-dimensional mechanical metamaterials or ‘meta-liquids’ have recently been fabricated. In contrast to normal liquids, anisotropic meta-liquids are also possible—a prerequisite for realizing many of the envisioned transformation-elastodynamics architectures. Here, we study several possibilities theoretically for introducing intentional anisotropy into three-dimensional pentamode metamaterials. In static continuum mechanics, the transition from anti-auxetic pentamode materials to auxetics is possible. Near this transition, in the dynamic case, approximately uniaxial versions of pentamode metamaterials deliver anisotropic longitudinal-wave phase velocities different by nearly a factor of 10 for realistically accessible microstructure parameters.

<sup>3</sup> Author to whom any correspondence should be addressed.



Content from this work may be used under the terms of the [Creative Commons Attribution 3.0 licence](http://creativecommons.org/licenses/by/3.0/). Any further distribution of this work must maintain attribution to the author(s) and the title of the work, journal citation and DOI.

## Contents

<b>1. Introduction</b>	<b>2</b>
<b>2. Anisotropy by moving <math>P</math> along the space diagonal</b>	<b>2</b>
<b>3. Anisotropy by moving <math>P</math> along the cubic axes</b>	<b>10</b>
<b>4. Conclusion</b>	<b>11</b>
<b>Acknowledgments</b>	<b>12</b>
<b>References</b>	<b>12</b>

## 1. Introduction

Normal liquids are hard to compress but easy to deform. Thus, their elastic bulk modulus is finite, while their shear modulus is negligible. This property makes wave propagation inside isotropic liquids fairly simple in that there is only one mode of propagation, i.e. longitudinal compression waves like for sound in air. The other five ('penta') possible shear-related transverse modes are absent or, formally, they have zero frequency [1, 2]. In this sense, liquids in three dimensions are pentamode materials. For an ideal isotropic pentamode material, the shear modulus is nearly zero, hence Poisson's ratio approaches +0.5 from below. In contrast, for an ideal three-dimensional isotropic auxetic material [3–5], the ratio of shear to bulk modulus tends to infinity; hence Poisson's ratio approaches  $-1.0$  from above. Thus, a pentamode material can be seen as an 'anti-auxetic'.

Following a theoretical suggestion by Milton and Cherkaev [6], pentamode materials can also be approximated by special three-dimensional solid microstructures. This idea opens up several new possibilities. Firstly, such microstructures do not 'flow away' and, thus, intentionally spatially inhomogeneous meta-liquids become possible. This aspect of tuning the local elastic wave parameters has recently been studied theoretically [20, 21]. Secondly, again in sharp contrast to normal liquids, such microstructures can be made intentionally anisotropic, i.e. the longitudinal wave velocity would depend on the propagation direction. Anisotropy is crucial for realizing several theoretical suggestions for transformation-elastodynamics [7–12] architectures by which, e.g., three-dimensional mechanical or acoustic free-space cloaks could become a reality. Experiments for the simpler two-dimensional case have been presented previously [13–19].

In their pioneering 1995 work [6], Milton and Cherkaev have also already suggested that pentamode metamaterials could, in principle, be made anisotropic. However, we are not aware of any study actually addressing this possibility quantitatively. The aim of the present paper is to fill this gap, i.e. to provide a guide to experimentalists as to what range of effective anisotropies is realistically accessible by adjusting the pentamode microstructure unit cell.

## 2. Anisotropy by moving $P$ along the space diagonal

Figure 1(a) exhibits the extended face-centered-cubic (fcc) unit cell of a pentamode metamaterial with lattice constant  $a$  for parameters corresponding to our recent experiments [20]. The structure is composed of double cones touching each other at their thin ends. These connection points form a diamond lattice, which is composed of two fcc

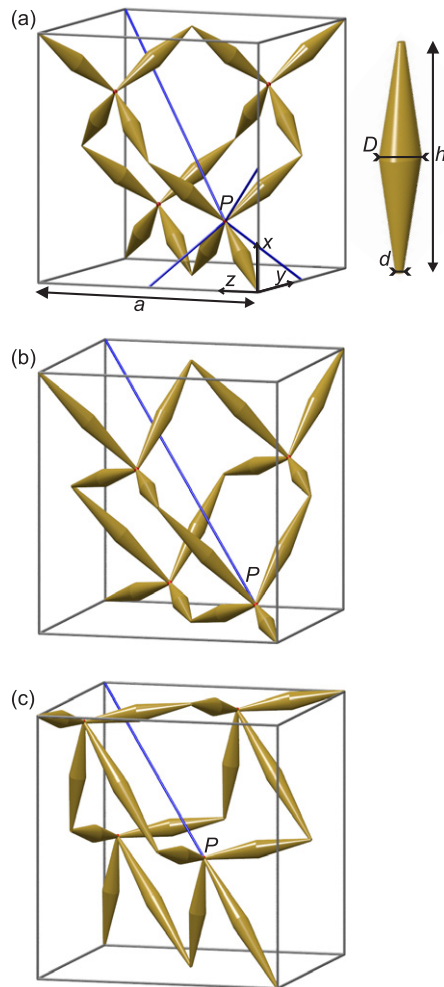


**Figure 1.** (a) The extended fcc unit cell of an isotropic pentamode metamaterial in which double cones touch at points forming a diamond lattice. The geometrical parameters correspond to our recent experiments [20]. We indicate the small diameter of the double cones  $d$ , their large diameter  $D$  and an fcc lattice constant of  $a$ . In the isotropic case, this leads to a double cone length of  $h = \sqrt{3}/4 a$ . For reference, the Cartesian  $xyz$  coordinate system used is also indicated at the lower right-hand side corner of the cube. In panel (a), as is usual for a diamond lattice, the connection point  $P$  corresponds to  $p = 25\%$ . Panels (b) and (c) illustrate two examples of anisotropic versions of pentamode metamaterials in which  $P$  has been moved along the space diagonal. (b)  $p = 15\%$  and (c)  $p = 42\%$ . This shifting leads to a reduced crystal symmetry and to more anisotropic wave propagation.

sub-lattices shifted with respect to each other by 25% of the cube's space diagonal along the space diagonal. This diamond lattice leads to isotropic wave propagation of longitudinally polarized (i.e. compression-like) modes in three dimensions [21]. It is clear that this diamond-like structure can be made more anisotropic in a large number of different ways. Milton and Cherkhaev suggested shifting one of the connection points, for example the point  $P$  in figure 1(a)

located at  $p = 25\%$  of the space diagonal of the fcc cube, along the space diagonal. This means that the point  $P$  has the Cartesian coordinates  $(pa, pa, pa)$ . In panel (b)  $p = 15\%$  and in (c)  $p = 42\%$ . Here, we have kept the diameter of the thin ends of the cones,  $d$ , and that of the thick parts,  $D$ , as well as the location of all other connection points within the primitive unit cell fixed. Of course, the length of all double cones does change upon moving  $P$ .

A convenient and relevant way of obtaining an overview of the resulting elastic behavior is to inspect the phonon band structure. All structural changes discussed in this paper leave the shape and size of the pentamode metamaterial primitive unit cell, hence the translational lattice, unaffected, but they do change the content of the primitive real-space unit cell and, thus, change the crystal symmetry. It is clear from the geometry that one can expect a different wave velocity for propagation along the fcc cube's space diagonal than for directions perpendicular to that axis. It is not obvious, however, how much anisotropy can be expected quantitatively. To calculate the phonon band structure, as in our previous work [21], we numerically solve the elastodynamic eigenvalue problem for the displacement vector  $\vec{u}$  by imposing Bloch-periodic boundary conditions onto  $\vec{u}$  with respect to the primitive fcc unit cell. We use the commercial finite-element software package Comsol Multiphysics. For a typical meshing, the maximum element size is  $0.025a$  and the minimum element size  $0.0008a$ . Typically, this leads to approximately  $10^5$  tetrahedra. All the resulting band structures depicted below have been checked for convergence. To allow for a direct connection to our previous work [20, 21], we use one specific set of parameters. For the constituent material, we choose Young's modulus as 3 GPa, Poisson's ratio as 0.4 and the mass density as  $1190 \text{ kg m}^{-3}$ . These parameters describe a typical polymer. For the geometrical structure parameters, we choose the small diameter  $d = 0.55 \mu\text{m}$  (see figure 1(a)), the large diameter  $D = 3 \mu\text{m}$  and an fcc extended unit cell lattice constant of  $a = 37.3 \mu\text{m}$ . In the isotropic pentamode metamaterial case, this lattice constant corresponds to a double cone length of  $h = \sqrt{3}/4a = 16.15 \mu\text{m}$ . However, as argued previously [21], the scalability of the elastodynamic equations allows us to easily translate these results to other size regimes and/or to different elasticities. For example, multiplying all geometrical parameters by a factor of 1000 decreases the absolute frequencies by 1000 and increases the wavelengths by 1000. Multiplying the elasticity tensor by, e.g., 100 increases the frequencies by a factor of 10. Poisson's ratio of the constituent material previously had very little if any influence and is thus kept constant in the present study.

Panels (a)–(c) of figure 2 depict calculated band structures for different positions of  $P$  on the fcc cube's space diagonal. The frequency is given in units of MHz on the right-hand side vertical scale and in more universal normalized units on the left-hand side vertical scale. Here,  $\lambda$  is the air wavelength for a standard air sound velocity of  $343 \text{ m s}^{-1}$  and  $a$  is the fcc lattice constant (see figure 1(a)). In each of panels (a)–(c), the left-hand side half shows wave vectors along the cube's space diagonal (i.e. the  $(1, 1, 1)$  direction) and the right-hand side wave vectors pointing along one particular orthogonal direction, i.e. the  $(-1, 1, 0)$  direction. For small wave numbers, the dispersion of the lowest branches can be well approximated by straight lines. Their slope multiplied by  $2\pi$  (to obtain angular frequencies  $\omega$ ) is the corresponding constant phase velocity. The corresponding fitted straight lines are also depicted in figure 2. The chosen line color encodes the polarization of the wave. Green color of a straight line indicates a transversely polarized mode and red color a longitudinally polarized mode. This polarization has been determined by inspecting the character of the underlying modes (not depicted; for comparison see figure 3 in [21]). Precisely, we calculate the dot and the cross product of the wave vector and the displacement vector, i.e.  $\vec{k} \cdot \vec{u}$  and  $\vec{k} \times \vec{u}$ , in the long-wavelength limit. Zero dot product

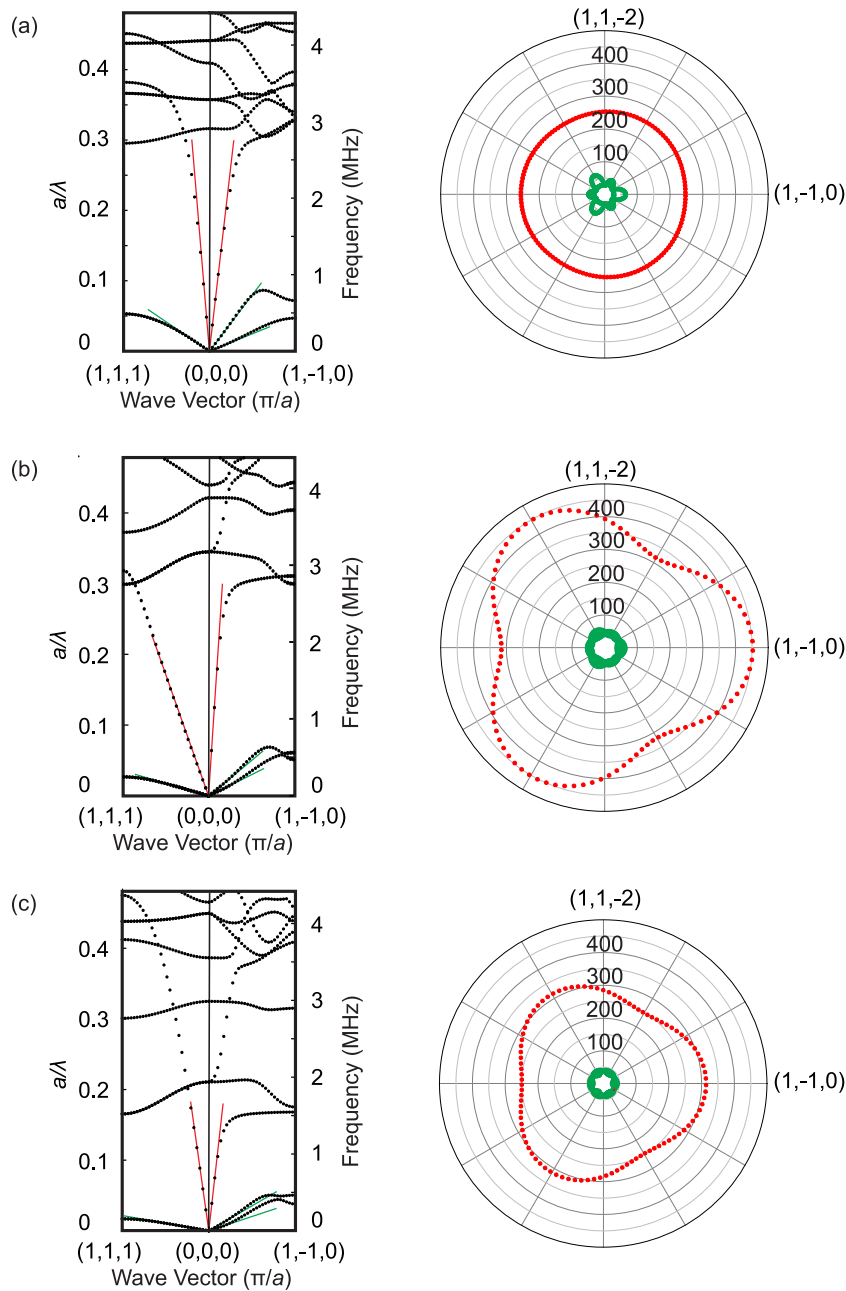


**Figure 2.** Left column: calculated band structures for three anisotropic pentamode structures (compare figures 1(b) and (c)). (a)  $p = 15\%$ , (b)  $p = 31\%$  and (c)  $p = 42\%$ . The straight lines are fits to the lowest dispersion branches in the long-wavelength (or small  $|\vec{k}|$ ) limit. Red (green) line color indicates a longitudinally (transversely) polarized mode. Right column: extracted phase velocities (in units of  $\text{m s}^{-1}$ ) in a plane normal to the fcc cube's space diagonal, i.e. the  $(1, 1, 1)$  direction. Red and green colors denote the polarization as before.

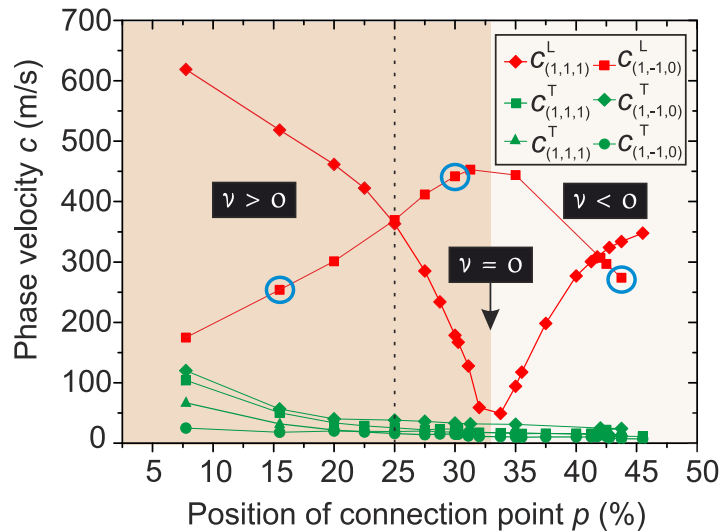


**Figure 3.** Phase velocities of longitudinally (red) and transversely (green) polarized modes as extracted from calculations like the ones shown in figure 2 as a function of the position of the point  $P$  along the fcc cube's space diagonal (compare figure 1). For the red-shaded region, the structure behaves like a pentamode metamaterial with positive Poisson's ratio, i.e.  $\nu > 0$ . At around a position of  $p = 33.3\%$ , the Poisson's ratio crosses zero, indicating a transition from a pentamode or anti-auxetic metamaterial to an auxetic metamaterial. This aspect is further illustrated in figure 4 for the static case and for parameters corresponding to the three blue circles.

indicates a transversely polarized mode and zero cross product a longitudinally polarized mode. Longitudinal polarization corresponds to a compression-like wave propagation like, e.g., for sound in air or in a liquid, and transverse polarization to a shear-like wave, which should be absent in an ideal liquid.

For applications in transformation elastodynamics, one might want uniaxial behavior, i.e. one phase velocity for propagation along a  $\bar{c}$ -axis and a different phase velocity that is the same for all perpendicular propagation directions. To investigate this aspect, the right-hand side column of figure 2 shows the phase velocities for propagation in a plane perpendicular to the cube's space diagonal in the form of a polar diagram. For an ideal uniaxial behavior, the red longitudinally polarized waves should appear as circles in the polar diagram. Obviously, we obtain nearly perfect circles for  $p = 15\%$  in figure 2(a), but deviations for the two other cases  $p = 31$  and  $42\%$  in panels (b) and (c) of figure 2, respectively. Possibly, one obtains circles in the limit of vanishing shear, i.e. in the limit of  $d/a \rightarrow 0$ . However, due to numerical constraints, we can presently not access yet smaller ratios of  $d/a$ . For an ideal meta-liquid, the green transversely polarized (shear-like) modes should have zero phase velocity. The green data in the right-hand side column of figure 2 indeed show that we have approached this ideal.

We have performed similar band-structure calculations for many other positions of the point  $P$  on the cube's space diagonal. The results are summarized in figure 3. Here, we plot the phase velocities  $c$  of the longitudinally polarized (index 'L' and again red color) and transversely polarized (index 'T' and again green color) modes for wave propagation along the cube's space diagonal  $(1, 1, 1)$  and for one selected perpendicular direction (as indicated in the legend). Note

that the case  $p = 1/3 \approx 33.3\%$  is a special geometry. At this point, three of the four double-cone elements within the primitive unit cell lie in one plane and the fourth double-cone axis is perpendicular to the other three. For  $p = 33.3\%$  numerical convergence of the complete band structure is difficult; hence we have rather chosen  $p = 31\%$  in figure 2. The data shown in figure 3 are converged around 33.3% however. When moving the position of the point  $P$  from  $p = 0$  to 33.3% (see the red shaded region), one longitudinal velocity decreases monotonically whereas the other one increases monotonically. The two curves obviously cross at  $p = 25\%$ , which corresponds to the diamond-type pentamode metamaterial. Above this point, the ratio of the two velocities becomes fairly large, while both branches are still reasonably well separated from the velocities of the green transversely polarized (shear-like) modes. Recall that these green branches should be at zero velocity for an ideal anisotropic artificial liquid. From an experimental viewpoint, the region between  $p = 25$  and 33.3% appears especially attractive. Herein, fairly small and easily realizable structure changes (also compare figure 1) induce significantly different longitudinal phase velocities. Toward the geometrically special case,  $p = 33.3\%$ , the ratio of the longitudinal-mode velocities approaches a factor of 10. However, at this point, the slower (red) longitudinal mode is no longer very well separated from the yet lower-velocity (green) transverse modes. Yet larger ratios are expected to be possible, in principle, by reducing the ratio of  $d/a$ , which, however, has already been  $0.55/37.3 \mu\text{m} \approx 1/68$  in figure 3. Significantly smaller ratios of  $d/a$  do not appear to be in reach experimentally and would also pose severe problems with respect to the convergence of the numerical band-structure calculations.

At  $p = 33.3\%$ , we find extrema for both red velocities versus the position of the point  $P$ , indicating a special mechanical behavior or a transition at this geometrically special point. To further investigate this aspect, we have performed additional static continuum-mechanics calculations. Following our previous work [20–22], again using the software package Comsol Multiphysics, we extract Poisson’s ratio for the three structures corresponding to the three blue circles in figure 3 that are below, near and above the transition point, respectively. The actual numerical calculations are based on pentamode structures composed of  $3 \times 3 \times 3 = 27$  extended fcc unit cells, equivalent to 108 primitive unit cells. The shown Poisson’s ratio corresponds to the average contraction (or extension) in the  $(1, 1, -2)$  direction when pushing along the  $(1, 1, 1)$  direction [22]. Note that for an anisotropic structure Poisson’s ratio depends on the pushing direction and turns into a tensor of rank 2 [23]. Mathematically, this corresponds to a  $3 \times 3$  matrix with all diagonal elements being  $-1$  by definition. Thus, the diagonal elements are not really physically meaningful Poisson’s ratios. The meaningful off-diagonal elements of the Poisson’s ratio tensor can lie outside the interval  $[-1.0, 0.5]$  for stable anisotropic structures [23, 24]. The results are visualized in figure 4, where only a part of the overall pentamode structure is shown in each case. For clarity, we have rotated the pentamode structure such that the fcc cube’s space diagonal in figure 1 corresponds to the vertical direction in figure 4 (also see coordinate systems in the middle). In panel (a)  $p = 15\%$ . Upon exerting a force along the vertical or  $(1, 1, 1)$  direction, the structure expands along the horizontal direction (see black arrows), meaning a positive Poisson’s ratio. In panel (b) for  $p = 31\%$ , very little horizontal expansion is found, corresponding to near-zero Poisson’s ratio (see black arrows). In panel (c), for  $p = 42\%$ , the horizontal contraction highlighted by the black arrows corresponds to a negative Poisson’s ratio. We conclude that the extremal phase velocities found in figure 3 around  $p = 33.3\%$  originate from the transition of the structure from a pentamode or anti-auxetic metamaterial to an auxetic metamaterial.

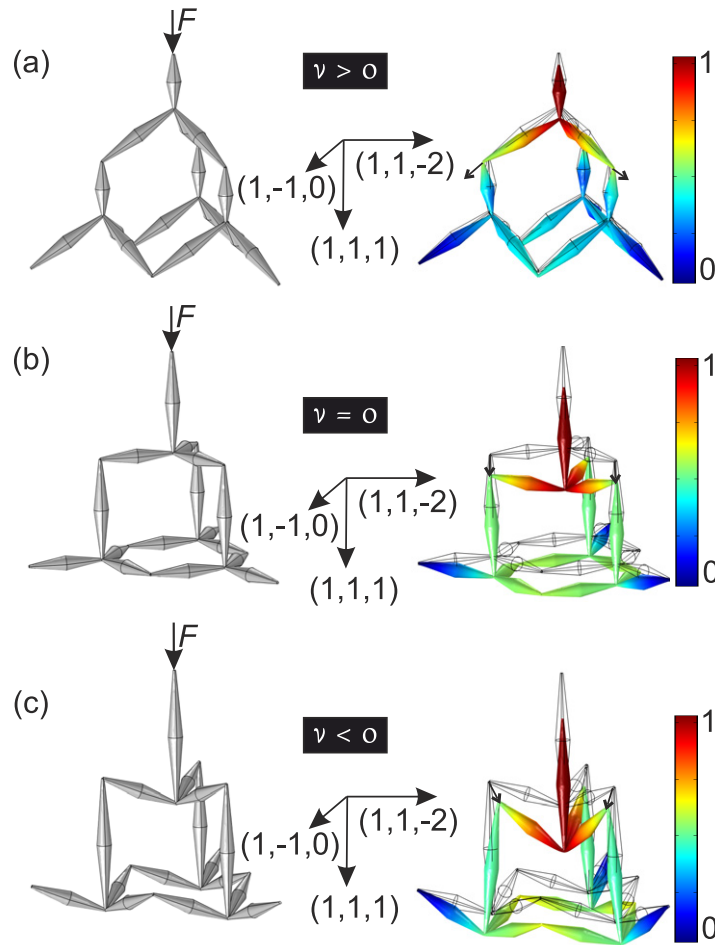


**Figure 4.** Illustrations of static continuum-mechanics calculations corresponding to the three configurations indicated by the three blue circles in figure 3, i.e. (a)  $p = 15\%$ , (b)  $p = 31\%$  and (c)  $p = 42\%$ . The left-hand side column depicts a characteristic part of the structure and the vertical pushing direction. Note that the coordinate system shown in the middle is rotated with respect to that used in figure 1. The right-hand side column shows the undistorted structure (hollow) and the structure distorted by the imposed stress on a false-color scale. The color at each point encodes the modulus of the displacement of that point in normalized units. Note that the displacement has intentionally been largely exaggerated. In contrast, the calculations have all been performed in the linear regime. Upon exerting a force  $\vec{F}$  as indicated, the structure expands along the horizontal direction in (a), does not move horizontally in (b) and contracts along the horizontal in (c). This indicates a Poisson's ratio  $\nu$  of (a)  $\nu = 0.9 > 0$  (anti-auxetic), (b)  $\nu = 0.1 \approx 0$  and (c)  $\nu = -0.4 < 0$  (auxetic).

At around  $p = 42\%$ , the two red curves in figure 3 cross again. Note, however, that the overall behavior is not really a crossing point; it is rather a crossing range, because the phase velocity for propagation perpendicular to the space diagonal is not constant. This can be seen from the corresponding red curves in the right-hand column of figure 2(c).

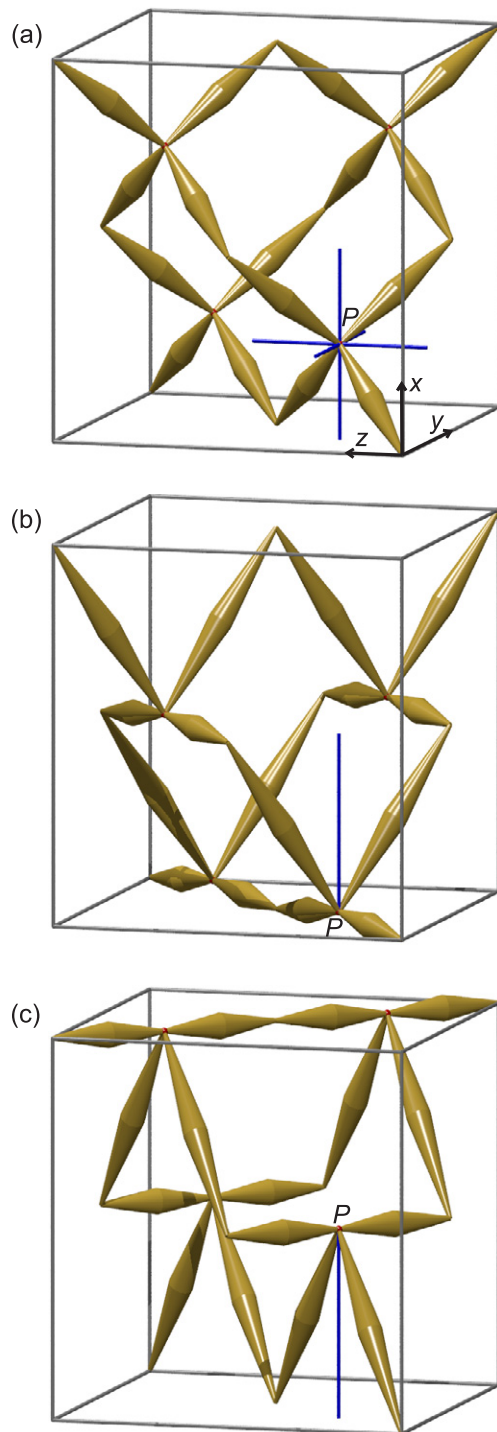


**Figure 5.** (a) Extended fcc unit cell of a pentamode metamaterial with lattice constant  $a$  like in figure 1(a) and  $p' = 25\%$ . Here, the  $x$  coordinate of the connection point  $P$  is at  $x = 25\% \times a$ . In panel (b)  $p' = 5\%$  and in panel (c)  $p' = 49\%$ .

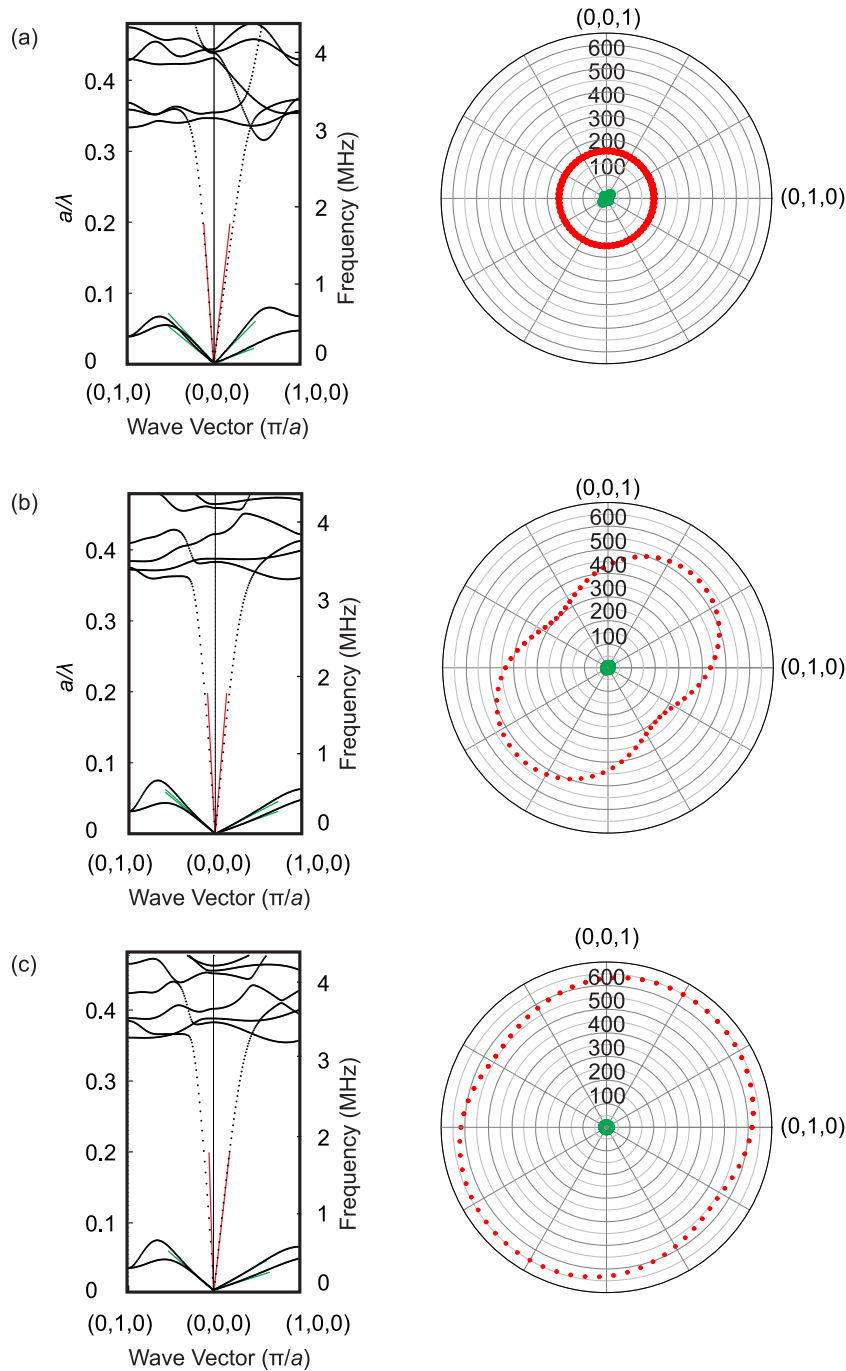


**Figure 6.** The same as figure 2, but the connection point  $P$  is shifted along the  $(1, 0, 0)$  direction instead of the  $(1, 1, 1)$  direction.  $P$  is placed at (a)  $p' = 14\%$ , (b)  $p' = 30\%$  and (c)  $p' = 42.5\%$ .

### 3. Anisotropy by moving $P$ along the cubic axes

Shifting the connection point  $P$  along the fcc cube's space diagonal as discussed in the previous section is just one out of infinitely many possibilities to make the isotropic pentamode metamaterial in figures 1(a) or 5(a) effectively anisotropic. In this section, we discuss a second

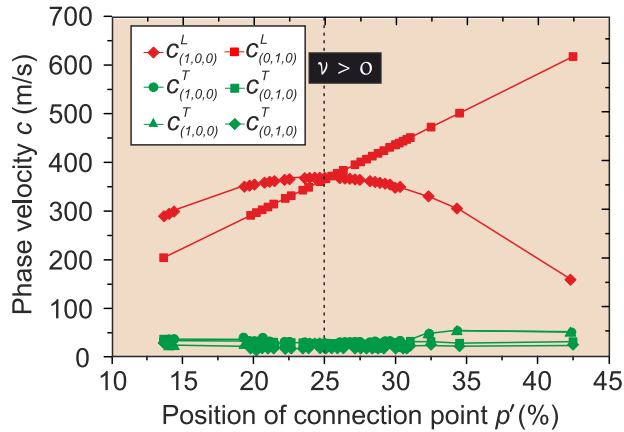


**Figure 7.** The same as figure 3, but the connection point  $P$  is shifted along the  $(1, 0, 0)$  direction instead of the  $(1, 1, 1)$  direction.

set of possibilities. We shift the connection point  $P$  in figure 1(a) along the  $x$  or  $(1, 0, 0)$  direction. This means that the point  $P$  has the Cartesian coordinates  $(p'a, 0.25a, 0.25a)$ . By symmetry, this is equivalent to shifting it along  $-x$  or along any of the other principal directions  $\pm y$  or  $\pm z$ . Two possible magnitudes of the shift are illustrated in panels (b) and (c) of figure 5. For reference, panel (a) repeats the regular pentamode metamaterial as in figure 1(a). The results depicted in figures 6 and 7 are the counterparts of those shown in figures 2 and 3 and discussed in the previous section. Broadly speaking, the effects of shifting  $P$  along  $(1, 0, 0)$  are less pronounced than for shifting it along the space diagonal  $(1, 1, 1)$ . The realistically accessible ratios of the (red) longitudinal phase velocities shown in figure 7 approach a factor of 4 near a position of 45%. While the (green) transverse velocities are yet smaller, the structure modifications are fairly drastic at this point already (compare figure 5(c)). Thus, this option appears less attractive to us compared to the shift along the space diagonal (the previous section).

We briefly mention that we have also investigated the possibility of leaving all double-cone connection points at their diamond positions but changing the diameter of the thin end of selected cones. The resulting anisotropies in the phase velocities of the longitudinal modes are yet smaller (not depicted). Furthermore, such a realization of anisotropy will likely be less tolerant to fabrication imperfections as the metamaterial behavior would depend on the precise shape of the tiny connection region. In contrast, the structure changes discussed in the previous section should be more robust against experimental fabrication imperfections.

#### 4. Conclusion

In conclusion, pentamode metamaterials can be seen as artificial fluids or meta-fluids for which the shear-like transversely polarized propagation modes have velocities that are small compared to those of the longitudinally polarized compression-like propagation modes. In contrast to normal liquids, pentamode metamaterials can be made intentionally spatially inhomogeneous and intentionally anisotropic with regard to the phase velocity of the compression-like modes. Here, we have calculated band structures of anisotropic versions of pentamode metamaterials for the first time. A systematic variation of parameters has been discussed. For realistically experimentally accessible parameters, the transverse phase velocities can be made different by

nearly an order of magnitude, while the smaller longitudinal velocity is still larger than all transverse velocities, but just by a factor of about 2 in the worst case. Yet larger anisotropy ratios may be desirable for implementing transformation elastodynamics architectures, e.g. three-dimensional free-space cloaks. Such larger anisotropies are possible in principle, but would require yet much smaller diameters of the double-cone connection regions of the pentamode metamaterials. In the present study, the connection diameter has already been nearly two orders of magnitude smaller than the lattice constant  $a$  of one extended fcc unit cell. The magnitude of the accessible mechanical property changes becomes especially prominent in the static limit. For example, upon moving just one connection point in the diamond lattice of connection points of double-cone elements along the space diagonal, a transition from an anti-auxetic to an auxetic metamaterial is induced.

## Acknowledgments

We thank Andreas Frölich, Aude Martin, Jonathan Müller and Michael Thiel (KIT) for stimulating discussions. We acknowledge support from the DFG-Center for Functional Nanostructures (CFN) via subproject A 1.5.

## References

- [1] Milton G W 2002 *The Theory of Composites* (Cambridge: Cambridge University Press)
- [2] Rand O and Rovinski V 2004 *Analytical Methods in Anisotropic Elasticity* (Basel: Birkhäuser)
- [3] Milton G W 1992 *J. Mech. Phys. Solids* **40** 1105
- [4] Greaves G N, Greer A L, Lakes R S and Rouxel T 2011 *Nature Mater.* **10** 823
- [5] Milton G W 2012 *J. Mech. Phys. Solids* at press (<http://dx.doi.org/10.1016/j.jmps.2012.08.011>)
- [6] Milton G W and Cherkaev A V 1995 *J. Eng. Mater. Technol.* **117** 483
- [7] Milton G W, Marc B and John R W 2006 *New J. Phys.* **8** 248
- [8] Norris A N 2008 *Proc. R. Soc. Am.* **464** 2411
- [9] Norris A N 2009 *J. Acoust. Soc. Am.* **125** 839
- [10] Brun M, Guenneau S and Movchan A B 2009 *Appl. Phys. Lett.* **94** 061903
- [11] Scandrett C L, Boisvert J E and Howarth T R 2010 *J. Acoust. Soc. Am.* **127** 2856
- [12] Gokhale N H, Cipolla J L and Norris A N 2012 *J. Acoust. Soc. Am.* **132** 2932
- [13] Cummer S A and Schurig D 2007 *New J. Phys.* **9** 45
- [14] Farhat M, Guenneau S and Enoch S 2009 *Phys. Rev. Lett.* **103** 024301
- [15] Popa B-I, Zigoneanu L and Cummer S A 2011 *Phys. Rev. Lett.* **106** 253901
- [16] Dupont G, Farhat M, Diattac A, Guenneau S and Enoch S 2011 *Wave Motion* **48** 483
- [17] Torrent D and Sánchez-Dehesa J 2011 *Wave Motion* **48** 497
- [18] Garcia-Chocano V M, Sanchis L, Diaz-Rubio A, Martinez-Pastor J, Cervera F, Llopis-Pontiveros R and Sánchez-Dehesa J 2011 *Appl. Phys. Lett.* **99** 074102
- [19] Stenger N, Wilhelm M and Wegener M 2012 *Phys. Rev. Lett.* **108** 014301
- [20] Kadic M, Bückmann T, Stenger N, Thiel M and Wegener M 2012 *Appl. Phys. Lett.* **100** 191901
- [21] Martin A, Kadic M, Schittny R, Bückmann T and Wegener M 2012 *Phys. Rev. B* **86** 155116
- [22] Bückmann T, Stenger N, Kadic M, Kaschke J, Frölich J, Kennerknecht T, Eberl C, Thiel M and Wegener M 2012 *Adv. Mater.* **24** 2710
- [23] Li Y 1976 *Phys. Status Solidi* **38** 171
- [24] Ting T C T and Chen T 2004 *Q. J. Mech. Appl. Math.* **58** 73